RESEARCH PAPER

F16357, a novel protease-activated receptor 1 antagonist, improves urodynamic parameters in a rat model of interstitial cystitis

Correspondence Nicolas Monjotin, Institut de Recherche Pierre Fabre, Castres, France. E-mail: nicolas.monjotin@pierre-fabre.com

N Monjotin[1], J Gillespie[2], M Farrié[1], B Le Grand[1], D Junquero[1] and N Vergnolle[3]

[1]Institut de Recherche Pierre Fabre, Castres, France, [2]Newcastle University, Newcastle upon Tyne, England, and [3]IRSD, Université de Toulouse, INSERM, INRA, INP-ENVT, Université de Toulouse-3 Paul Sabatier, Toulouse, France

BACKGROUND AND PURPOSE

The aims of the present study were to characterize the role of PAR1 in rat bladder under inflammatory conditions and determine whether a selective PAR1 antagonist, F16357, can prevent the pathophysiological symptoms of cyclophosphamide-induced interstitial cystitis (IC).

EXPERIMENTAL APPROACH

Immunohistochemistry, contractile activity in isolated bladder and urodynamics were determined before and after cyclophosphamide treatment. F16357 was administered intravesically during the acute phase of inflammation, and effects on PAR1 and PAR1-related bladder contraction evaluated 24 h after cyclophosphamide injection. Urodynamics and associated voided volumes were recorded 7 and 24 h after cyclophosphamide.

KEY RESULTS

In control conditions, PAR1 was present only in some umbrella cells. Cyclophosphamide disrupted the urothelium and expression of PAR1 by all remaining urothelial cells. After F16357 treatment, urothelial damage was absent and PAR1 immunoreactivity similar to control tissues. Thrombin and TFLLR-NH$_2$ induced bladder contractions. These were increased in inflammatory conditions and antagonized by F16357 in a concentration-dependent manner. In telemetric experiments, furosemide increased urine production and voiding frequency for 60 min, 7 h after cyclophosphamide injection. Intravesical administration of F16357 blocked these changes with a return to a physiological profile; 24 h after cyclophosphamide, the volume of micturition was still lower with no increase in number of micturitions. F16357 30 μM reduced the number of micturitions and improved bladder capacity, but did not affect diuresis. Under similar experimental conditions, lidocaine 2% induced comparable effects.

CONCLUSIONS AND IMPLICATIONS

PAR1 is expressed in rat bladder, overactivated in inflammatory conditions and involved in bladder function and sensation. F16357 could represent an interesting candidate for IC treatment.

Abbreviations

A, amplitude of micturition; BP, basal pressure; BPS, bladder pain syndrome; CYP, cyclophosphamide; IC, interstitial cystitis; ICI, inter-contraction interval; IR, immunoreactivity; MIF, macrophage migration inhibition factor; MP, micturition pressure; SRE, serum response element; T, time of injection; TBS, Tris-buffered saline; TBS-T, TBS-Tween; V, voided volume per micturition

Tables of Links

TARGETS	
GPCRs[a]	Enzymes[b]
PAR1	COX1
PAR2	Neutrophil elastase
PAR3	Neuronal NOS
PAR4	

LIGANDS	
Acrolein	Lidocaine
Cyclophosphamide	TFLLR-NH$_2$
Furosemide	Thrombin
GTPγS	

These Tables list key protein targets and ligands in this article which are hyperlinked to corresponding entries in http://www.guidetopharmacology.org, the common portal for data from the IUPHAR/BPS Guide to PHARMACOLOGY (Southan *et al.*, 2016) and are permanently archived in the Concise Guide to PHARMACOLOGY 2015/16 ([a,b]Alexander *et al.*, 2015a,b).

Introduction

The main roles of the urinary bladder are storage of urine and voiding at socially convenient moments. Several pathological situations such as interstitial cystitis (IC) and bladder pain syndrome (BPS) are characterized by pelvic pain, inflammation and detrusor dysfunction. The symptoms of IC and BPS constitute a number of idiopathic heterogeneous disorders with unknown cause that are manifest as increased urinary frequency and urgency (Hanno *et al.*, 2015). Unfortunately, at the present time, there is no effective treatment for these diseases.

Cyclophosphamide (CYP)-induced cystitis is a well-established experimental model of bladder inflammation and dysfunction due to the accumulation of its metabolite acrolein and damage to the urothelium in the bladder (Cox, 1979). In rats, an acute i.p. injection of CYP induces signs of pelvic pain (Saitoh *et al.*, 2010), inflammation (Lecci *et al.*, 2000; Auge *et al.*, 2013) and alterations in urodynamic parameters (Hu *et al.*, 2005; Dornelles *et al.*, 2014). Importantly, this acute model demonstrates many features of IC in humans. We have recently described a telemetric approach to evaluate, in the same conscious animal, urodynamic parameters in control conditions and after CYP injection (Monjotin *et al.*, 2016). We now use this approach to evaluate drugs acting on lower urinary tract dysfunctions induced by CYP.

Protease-activated receptors (PAR1, PAR2, PAR3 and PAR4) are a unique class of receptors that carry their own ligands tethered to the receptor complex. The protease cleaves the N-terminal part and allows receptor self-activation. Among these, the PAR1, a GPCR, is activated by proteolytic cleavage of the N-terminus by thrombin and trypsin (Dery *et al.*, 1998). Some studies have shown that CYP induces an increased expression and function of the PARs in bladder (Dattilio and Vizzard, 2005; Moffatt, 2007).

Proteases released during bladder inflammation play a key role in the urinary system and hyperalgesia in rodents, and a deficiency of PAR1 expression reduced bladder inflammation (D'Andrea *et al.*, 2003; Saban *et al.*, 2007). The intravesical administration of PAR-activating peptides results in a local inflammatory reaction (Saban *et al.*, 2007), and thrombin stimulates the release of macrophage migration inhibitory factor (MIF), a pro-inflammatory cytokine, by urothelial cells (Vera *et al.*, 2010).

Consequently, PARs seem to be involved in bladder dysfunctions. The involvement of PAR2 has been extensively studied (Moffatt, 2007). However, a definitive role for PAR1 in IC physiopathology and associated bladder dysfunctions has yet to be established in functional models of lower urinary tract syndromes.

The aims of the present study were to characterize the roles of PAR1 in rat bladder under inflammatory conditions and determine whether a selective PAR1 antagonist, namely, F16357, can prevent the pathophysiological alterations in CYP-induced IC.

Methods

Compliance with requirements for experimental design, statistical analysis and requirements for studies using animals

Seventy-six adult female rats (Sprague Dawley or Wistar Han, 200–250 g; Charles River, l'Arbresle, France) were kept, at least two per cage (polysulfone type 1291H with shaving litter), at a constant temperature (22 ± 2°C), with controlled humidity (40–70%), controlled ventilation (more than 10 changes h^{-1}) and a regular light/dark cycle (12 h/12 h, 07 h to 19 h), with food and tap water provided *ad libitum*. Animals were acclimatized to their conventional environment for at least 5 days after their arrival. Music was broadcasted in all animal facilities and enrichment such as toys or cotton was given when compatible with the experiments.

All animal care and experimental procedures were in accordance with the 2010/63/EU Directive on the protection of animals used for scientific purposes and French legislation decree n° 2013–118 and were approved by the internal Ethic committee (CEA-CEPC-110 approved on March 16, 2013). The experimental procedures used in the work described in this article were as humane as possible. Animal studies are reported in compliance with the ARRIVE guidelines (Kilkenny *et al.*, 2010; McGrath & Lilley, 2015).

CYP-induced IC is a well-described model, and most of the bibliography on this model is on mouse and rats. Bladder telemetry has already been studied in rats and justifies the selection of rats for these studies. Moreover, this work and especially the *in vivo* experiments rely on previously described experiments on bladder pressure evaluation by telemetry in

rats. In all these experiments, no analgesia was given to the animals after CYP injection because evaluation of the effects of compounds was essentially based on bladder function related to sensation/pain. Nevertheless, a behavioural evaluation of the pain was performed regularly (presence of ptose, chromodacryorrhoea, hunched back, abdominal licking and/or piloerection) to ensure that internal critical end points were not exceeded and in compliance with ethical procedures. Moreover, animals were placed under a heating lamp for at least 4.5 h after CYP injection to avoid CYP-induced hypothermia. No animals had to be killed due to ethical issues.

The rationale for the chosen group size, to obtain a representative evaluation of pharmacological effect of tested compounds, was evaluated by a statistician and approved by the internal ethical committee. For preliminary *in vitro* experiments related to immunohistochemistry, in which no statistical analysis was performed, only three animals per condition were used, with a total of $n = 9$ animals. For other experimental conditions, the number of animals used is presented in figure legends. In organ bath chamber experiments, at least one strip was treated with vehicle on each day of the experiment to ensure the reproducibility of the test, thus explaining the difference in group size between F16357-treated strips and vehicle-treated strips in both physiological and inflammatory conditions. The difference in group size observed between physiological and inflammatory conditions in organ bath chamber experiments was related to the anticipation of a major impact of CYP on animal welfare below the end points at which the animals would need to be killed. However, no animals reached these end points, and the supplementary strips were included in the results. In the telemetric experiments, the difference in group size was due to a loss of bladder pressure signal. Randomization of animals was performed on body weight for *in vitro* experiments. No randomization was performed for telemetric experiments because the animals were reused for different groups.

Data were not recorded blindly, but analyses were. Experiments and audit were carried out in a quality environment assessed by regular audits conducted by the quality assurance unit and in respect of internal standard operating procedures.

Study design

In vitro evaluation of F16357 in PAR1-overexpressed conditions

Determination of ligand efficacy by [^{35}S]-GTPγS binding assay in COS-7 cells transiently expressing human PAR1. Receptor-linked G protein activation of PAR1 was determined by measuring the stimulation of [^{35}S]-GTPγS (1000 Ci·mmol^{-1}) incorporation, essentially as previously described (Wurch *et al.*, 1999). Briefly, COS-7 cells were transiently transfected with pRK5-PAR1 plasmid, coding for the human PAR1, by electroporation. Membranes of COS-7 cells expressing human PAR1 were pre-incubated 30 min with F16357 alone or in the presence of TFLLR-NH$_2$ (3 μM) in a buffer containing 20 mM HEPES (pH 7.4), 0.1 μM GDP, 3 mM MgCl$_2$ and 100 mM NaCl. The reaction was started with 0.4 nM [^{35}S]-GTPγS in a final volume of 500 μL in 96-well

plates, and incubation was performed for an additional 30 min. Experiments were terminated by rapid filtration, and counting was performed using a Topcount microplate scintillation counter (Perkin-Elmer). Basal binding is defined as 0%. Efficacy is expressed relative to [^{35}S]-GTPγS binding stimulated by 10 μM TFLLR-NH$_2$ (=100%), and antagonist potency was determined against TFLLR-NH$_2$ (3 μM)-induced [^{35}S]-GTPγS binding.

Serum Response Element (SRE)-dependent luciferase activity in COS-7 cells expressing human PAR1. COS-7 cells were co-transfected with plasmid expressing human PAR1 (1 μg) and the SRE-luciferase reporter gene (5 μg), seeded in 96-well plates, and luciferase activities were measured 48 h post-transfection in serum-deprived cells as previously described (De Vries *et al.*, 2006). F16357 was added 15 min before the 5 h agonist treatments. Luminescence was detected in a Topcount luminometer (Perkin-Elmer) and expressed as a percentage of TFLLR-NH$_2$ (1 μM)-induced SRE-luciferase response.

Immunohistochemistry experiments

CYP, 150 mg·kg^{-1}, or its vehicle (saline) was injected bilaterally i.p. in a final volume of 5 mL·kg^{-1} to induce bladder inflammation (T = 0). At T + 2.5 h, animals were anaesthetized by isoflurane 1.5% (0.5 L·min^{-1} per animal), and the bladder was emptied. A catheter (PE-10) was inserted in the bladder through the urethra, and the intravesical administration of saline was performed. The urinary meatus was clamped, and the catheter was removed. After 60 min of exposure, the clamp was removed, the bladder was emptied and the animals were returned to their home cage to recover. Animals were placed under a heating lamp after the CYP injection for up to 4.5 h in order to avoid CYP-induced hypothermia; 24 h after CYP injection, the animals were anaesthetized with pentobarbital (60 mg·kg^{-1}, 1 mL·kg^{-1}) and killed by cervical dislocation and the bladders excised and fixed for 2 h in 4% paraformaldehyde in PBS. The bladders were then washed in PBS and transferred to solutions with progressively higher sucrose concentrations (10, 20 and 30%) to act as a cryo-preservant. The tissues were subsequently 'snap-frozen' using isopentane. Tissue sections (7–8 μm) were cut at −25°C, placed on polylysine-coated slides and air-dried. Sections were washed in Tris-buffered saline (TBS), TBS Tween (TBS-T) and subjected to a TBS wash cycle for 5 min at each stage. Primary antibodies were diluted with PBS with 1% triton-X. Combinations of primary antibodies were then placed on each slide and incubated overnight at 4°C. Primary polyclonal antibodies included were against PAR1 (1:100; Santa Cruz, Cat No. sc-8202), vimentin (1:5000; BioGenex, Cat. No MU074-uc), COX1 (1:100; Santa Cruz, Cat No. sc-1752) and neuronal NOS (1:500; Santa Cruz, Cat. No. 648) were used. These antibodies were chosen because they have been characterized at the molecular level for the specific epitope (see manufacturers data sheets). After overnight incubation, sections were washed in TBS, TBS-T and TBS and incubated with appropriate secondary fluorescent antibodies: mouse, goat and rabbit primary antibodies were visualized using donkey anti-mouse/goat/rabbit IgG antibody conjugate (Molecular Probes) Alexa Fluor 488 or 594 for 1 h at room temperature. Slides were then washed, a drop of Vectashied/DAPI was added, and covered with a cover slip.

Sections were viewed using an Olympus BX61 fluorescence microscope with ×10, ×20 and ×60 objectives. Images were captured using an Olympus XM10 monochrome camera in 16-bit digital format and examined using Image J software (National Institutes of Health).

Isolated bladders contractility

At T0, CYP or its vehicle was administered as previously described; 24 h after CYP injection, animals were anaesthetized with pentobarbital (60 mg·kg^{-1}, 1 mL·kg^{-1}) and killed by cervical dislocation. The urinary bladder was promptly removed and placed in oxygenated modified Krebs–Henseleit solution of the following composition (mM): NaCl 114, KCl 4.7, CaCl$_2$ 2.5, MgSO$_4$ 1.2, KH$_2$PO$_4$ 1.2, NaHCO$_3$ 25 and glucose 11.7 (pH 7.4, oxygenated with 95% O$_2$ and 5% CO$_2$). The bladder was cleaned of connective tissue, the distal and proximal portions were removed and the bladder was cut longitudinally in two equal strips. The strips were immersed in glass organ baths containing the oxygenated Krebs–Henseleit solution maintained at 37°C.

After an initial stabilization period of at least 90 min at a basal resting tension of 1.0 g, strips were exposed to KCl 50 mM to verify viability. After further stabilization and washing, one concentration of F16357 or vehicle (DMSO 0.3%) was added to the bath for 30 min. Then, a cumulative concentration–response curve or the response to a single administration of TFLLR-NH$_2$ (a selective PAR1-activating peptide) and/or thrombin (a native PAR1 protease) was performed.

In vivo experiments

Telemetric devices. The transmitters used for these experiments were PhysioTel HD-S10 (Data Science International), allowing pressure (accuracy ±3 mmHg) and activity measurements to be obtained in small animals (4.4 g and 3.1 cc). The pressure of each transmitter was calibrated at 3 points by the manufacturer. Calibration values were checked at three points (0, 30 and 100 mmHg) by a sphygmomanometer just before implantation and after the animal had been killed to ensure the validity of the data obtained.

Surgical procedure. Pre-operative analgesic (buprenorphine and ketofen) and antibiotic (enrofloxacin) treatments were given to all animals before anaesthesia (isoflurane 2–4%). In aseptic conditions, a small laparotomy was performed. The transmitter was placed on the right side of the abdominal cavity and sutured on the abdominal wall (silk 4/0) in order to avoid contact with the bladder. The pressure transducer was inserted in the dome of the urinary bladder and secured with a purse string (silk 6/0). After checking the pressure values, the incisions were closed with resorbable sutures (Vicryl 3/0 for abdominal wall and Vicryl 4/0 for skin). Animals received post-operative care (analgesic and antibiotic) for 2 days following the surgery. All animals were given a further recovery period of at least 1 month before being used for the experiments.

Before cystometric analyses, all instrumented rats were acclimatized to the experimental environment and basal urodynamic parameters established for all telemetered rats using a furosemide challenge as described previously (Monjotin *et al.*, 2016).

Measurement of urodynamic parameters by telemetry. Naïve instrumented rats received an injection of furosemide (Lasilix®10 mg·kg^{-1}, 2 mL·kg^{-1}, s.c.) to stimulate diuresis and were immediately placed in customized metabolic cages. Bladder pressure and voided volumes were continuously recorded for 60 min following the furosemide pulse. Cystometric evaluation was performed on conscious freely moving rats, and parameters recorded were micturition pressure (MP), basal pressure (BP), amplitude of micturition (A = MP-BP), inter-contraction interval (ICI) and voided volume per micturition (V).

After a washout period, another set of experiments was performed on the same animals. At T0, CYP 150 mg·kg^{-1} or its vehicle (saline) was administered. At T + 2.5 h, animals were anaesthetized using isoflurane 1.5% (0.5 L·min^{-1} per animal), and the bladder was emptied by gentle pressure on the abdominal wall. A catheter (PE-10) was inserted in the bladder through the urethra, and the intravesical administration of saline, F16357 30 μM or lidocaine 2% was performed. The urinary meatus was lightly clamped, and the catheter was removed. After 60 min, the clamp was removed, the bladder was emptied and the animals were returned to their home cage. The furosemide protocol was performed 7 and 24 h after CYP injection, and bladder pressure and voided volumes were continuously recorded as previously described. After the second furosemide evaluation, animals were anaesthetized with pentobarbital (60 mg·kg^{-1}, 1 mL·kg^{-1}) and killed by cervical dislocation. Then, each transmitter was removed and the pressure calibration checked.

Data and statistical analysis

Results are expressed as mean ± SEM, with *n* indicating the number of animals, strips or independent *in vitro* experiments used for a particular set of experiments. For *in vitro* experiments in recombinant models, isotherms were analysed by a nonlinear regression (Prism, GraphPad) to yield IC$_{50}$ values. K_b values of antagonists for inhibition of agonist action were calculated according to Lazareno and Birdsall calculation: $K_b = IC_{50}/\{1 + [(agonist)/EC_{50}]\}$ (Lazareno and Birdsall, 1993), where [agonist] is the concentration of TFLLR-NH$_2$ in the test (Lazareno and Birdsall, 1993). Values given are from at least five independent experiments performed at least in duplicate for [^{35}S]-GTPγS experiments and quadruplicate for SRE-luciferase experiments.

Statistical analysis of data was carried out using SigmaStat 3.5 software (Systat). For isolated bladder experiments, a two-way ANOVA followed by a multiple comparison versus vehicle with the Holm–Sidak method was performed only if F achieved $P < 0.05$, and there was no significant variance in homogeneity. For telemetric experiments, Student's paired *t*-test and Mann–Whitney rank sum test were used. Values of $P < 0.05$ were considered to show significant differences between means. The data and statistical analysis comply with the recommendations on experimental design and analysis in pharmacology (Curtis *et al.*, 2015).

Equipment

Isolated bladder contractions. For isolated bladder experiments, tissues were placed in organ bath chambers (EMKA Technologies). Isometric tension transducers (IT50, EMKA Technologies) were connected to amplifiers, (EMKA

Technologies) and contractile responses were recorded using IOX2 software (EMKA Technologies).

In vivo experiments. Telemetry equipment (Data Science International) was interfaced with easyMATRIX and IOX2 (EMKA Technologies). HD-S10 telemetry transmitters were used in conjunction with RPC-1 receivers. For volume measurements, customized IT50 isometric transducers (EMKA Technologies) were used. Weighing signals were converted through an analogue-to-digital IT50 converter (EMKA Technologies). For telemetric, cystometric and voided volume recording, animals were freely moving in customized metabolic cages (Technilab).

Drugs

CYP, lidocaine, thrombin, TFLLR-NH$_2$ and all reagents for buffer preparation were obtained from Sigma Aldrich. [^{35}S]-GTPγS was obtained from Perkin-Elmer Life Science and furosemide (Lasilix®) from local pharmacy.

F16357 (3-(2-chlorophenyl)-1-[4-(4-fluorobenzyl)-piperazin-1-yl]-propenone) was synthesized in a medicinal chemistry department at Pierre Fabre Research Institute.

Materials used for surgical procedures were obtained from Centravet.

Results

In vitro evaluation of F16357 in PAR1-overexpressed conditions

In a [^{35}S]-GTPγS binding assay at human PAR-1 thrombin receptors, F16357 had no agonist activity when tested alone (data not shown), but antagonized 3 μM TFLLR-NH$_2$-induced [^{35}S]-GTPγS binding with pKb values of 6.04 (5.61–6.82) (Figure 1A). In a standard SRE-luciferase reporter gene assay in PAR-1 transfected in COS-7 cells, F16357 antagonized 1 μM TFLLR-NH$_2$-induced luminescence with a pKb value of 5.49 (5.45–5.65) (Figure 1B).

Collectively, these results demonstrated that F16357 exerts an antagonism against PAR1 in various models with a pharmacological potency between 5.49 and 6.04 depending on the level of receptor expression. All these results are in accordance with those previously reported in the publication of Perez *et al.* (2009), in which compound #39 represents the F16357.

PAR1 immunoreactivity (IR) in the lateral wall of the bladder

Sections of the lateral wall of the bladder were examined for PAR1 IR after treatment with either vehicle (Figure 2A, control) or CYP (Figure 2B). In control rats, the urothelium, stained with an antibody to NOS [green appears as a multilayered structure, arrows: (+)]. PAR1-IR can be seen (red), but this is localized to the umbrella cells. Not all umbrella cells were PAR1-IR with large areas showing no PAR1-IR. No PAR1-IR was detected in cells of the lamina propria or muscle layer; 24 h after CYP treatment, there was a clear disruption and damage to the urothelium (Figure 2B). Cells of the urothelium have been lost, and the barrier is absent or reduced to a single-cell layer. Such changes are often associated with an expansion
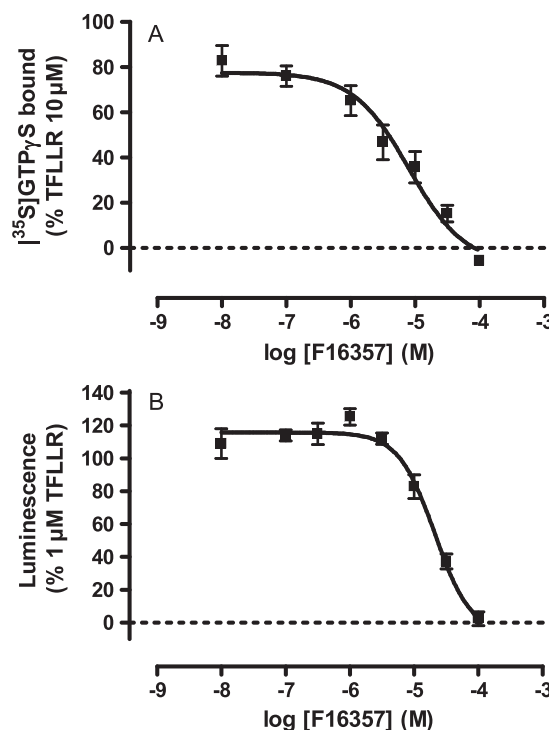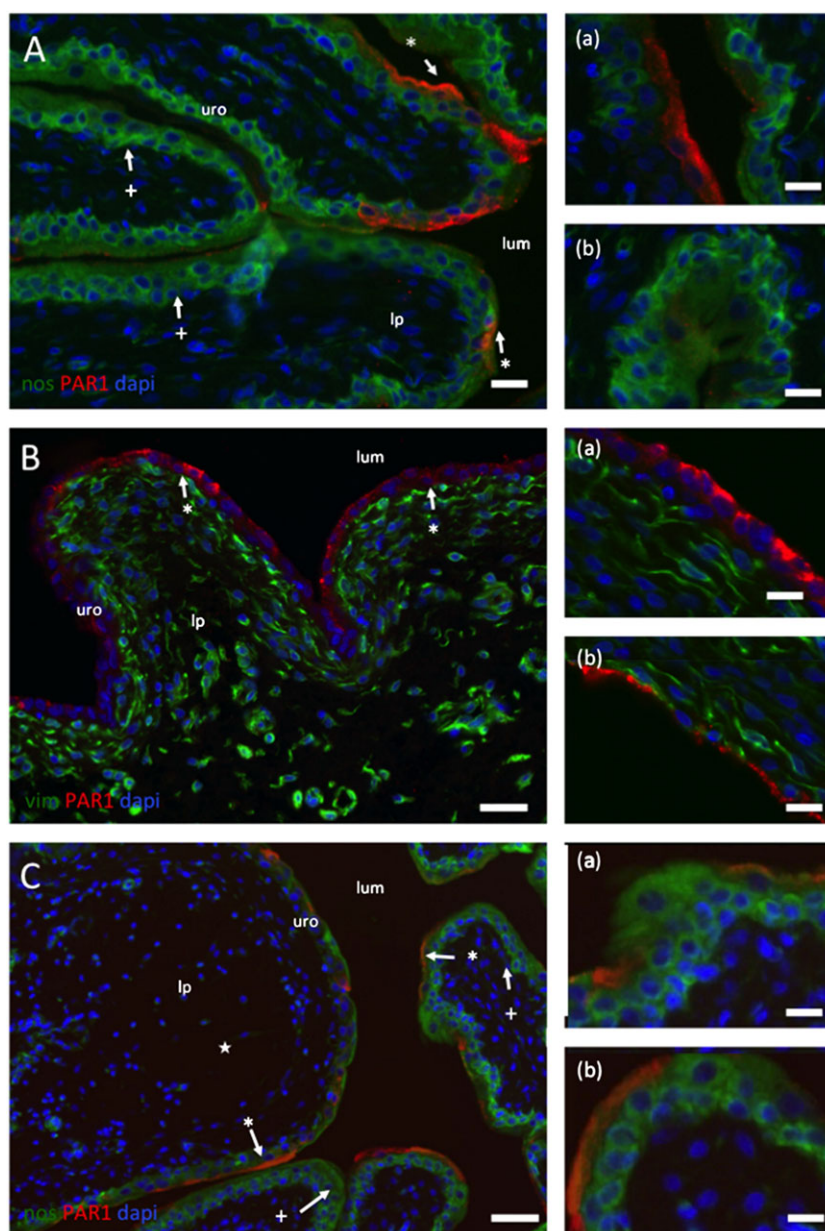

Figure 1

Concentration-dependent effect of F16357: on TFLLR-NH$_2$-induced G-protein activation ($n = 5$ independent experiments) (A) or on TFLLR-NH$_2$-induced SRE-luciferase activity ($n = 5$ independent experiments) (B); both in the membrane of COS-7 cells.

of the lamina propria, but there appears to be little damage to the sub-urothelial interstitial cells. All of the urothelial cells remaining after CYP were strongly PAR1-IR. The 'punctate' distribution was lost. Qualitatively, these observations suggested an increased expression of PAR1 in the basal urothelial cells after CYP exposure. Intravesical administration of F16357 (30 μM) 2.5 h after CYP treatment appeared to induce less damage (Figure 2C). PAR1-IR was again restricted to a small population of umbrella cells. Note that, however, in the section illustrated, the lamina propria was still expanded (Figure 2C). Therefore, the local administration of F16357 appeared to prevent the sequence of events underpinning urothelial damage possibly by preventing the overexpression and activation of PAR1.

Effect of PAR1 activation in the bladder

Typical traces, demonstrating a concentration-dependent increase in the amplitude of micro-contractions evoked by the PAR1-selective activating peptide TFLLR-NH$_2$, are shown in Figure 3A, B. In physiological conditions, the amplitude of these contractions was <0.1 g and increased up to 0.7 g 24 h after CYP treatment. In both physiological and inflammatory conditions, pretreatment with F16357 30 μM suppressed the maximal contraction elicited by TFLLR-NH$_2$ (Figure 3C, D) and reduced the rhythmic instability. A specific analysis based on an evaluation of the AUC of micro-contractions showed that these micro-contractions were reduced by 48% after F16357 (30 μM) treatment (Figure 3D).
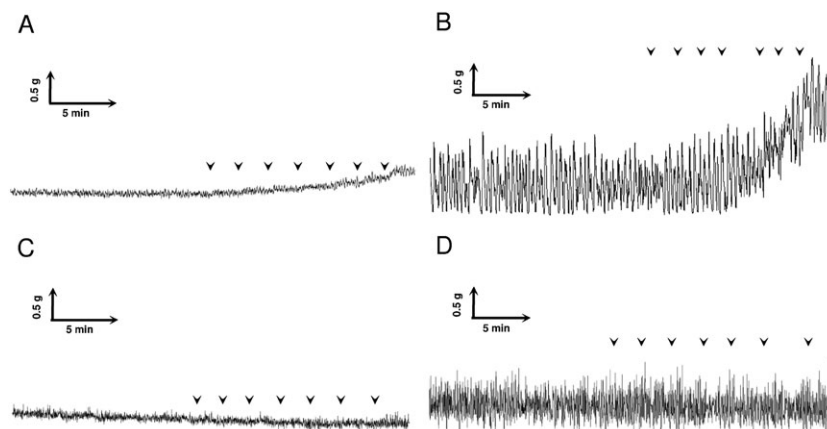
Figure 2

Location of IR to PAR1 in control (A), CYP-treated (B) and CYP + F16357-treated bladders. (A) Sections of the lateral wall of the bladder from a control rat illustrating the regionalized localization of IR to PAR1 (red) to primarily the umbrella cells of the urothelium (*). The lumen (lum), urothelium (uro) and *lamina propria* are identified. Regions of the urothelium devoid of PAR1-IR are also apparent (+). The section is counterstained with an antibody to NOS (green) and the nuclear marker DAPI (blue). Calibration bars (A), (B) and (C) 30 mm. (B) Sections of lateral wall from a rat injected with CYP. Note (a) the disruption and loss of the urothelium down to a single cell layer and (b) the appearance of PAR1-IR in all epithelial cells. No PAR1-IR was found in the *lamina propria* interstitial cells. These sections are also stained with an antibody to vimentin (Vim: green) to identify interstitial cells. Calibration bars (B) 40 and 15 mm in (a) and (b). (C) Images from bladders from CYP-treated animals that also had intravesical F16357 (30 μM). The section is counterstained with an antibody to NOS (green) and the nuclear marker DAPI (blue). Note the absence of urothelial damage and the regional distribution of PAR1-IR to the umbrella cells. Also, a region of the bladder wall where the *lamina propria* has expanded (★). Calibration bars (C) 100 mm, (a) 20 and (b) 15 mm.
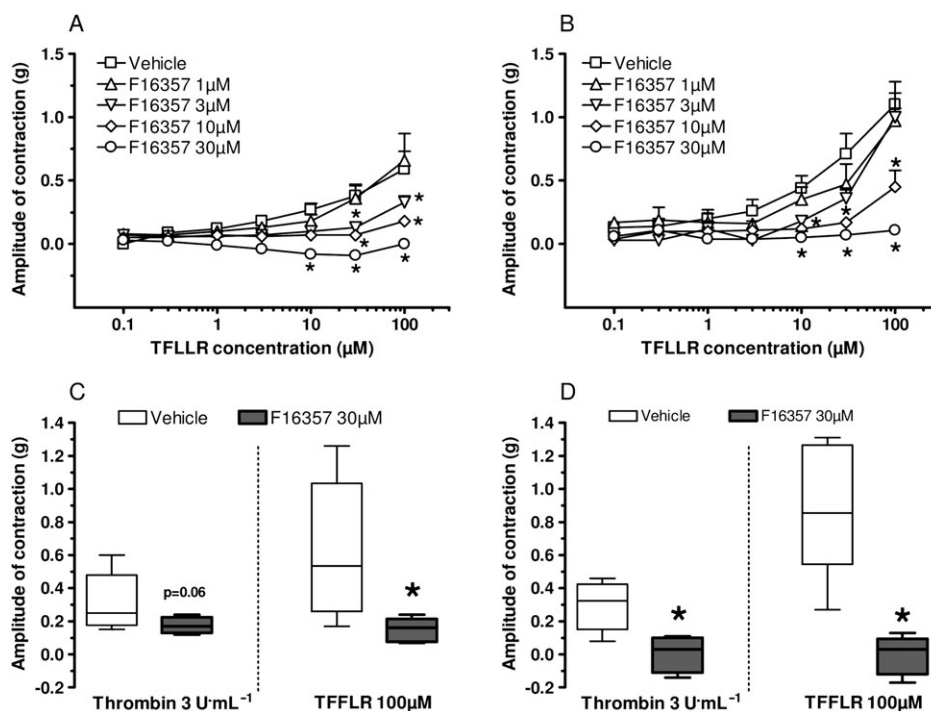
Under control conditions, TFLLR-NH$_2$ induced concentration-dependent contractions from 1 μM (threshold) up to 100 μM, and the maximal amplitude was about 0.6 g (corresponding to 14% of KCl 50 mM contraction). F16357 decreased the TFLLR-NH$_2$-induced bladder contraction in a concentration-dependent manner with a total

blockade at 10 and 30 μM ($P < 0.05$ for both) (Figure 4A). These results demonstrate that the PAR1 was involved in the generation or modulation of micro-contractions in the isolated bladder; 24 h after CYP treatment, TFLLR-NH$_2$ induced concentration-dependent contractions of bladder strips from 1 μM (threshold) up to 100 μM. The maximal

Figure 3

Representative traces of *in vitro* bladder contraction recording. Effect of cumulative concentration–response curve with TFLLR-NH$_2$ (1×10^{-7} up to 1×10^{-4} M in semi-logarithmic increment, each arrow represents one concentration) in physiological conditions (A) and 24 h after CYP injection (B). Effect of F16357 (30 μM) on the cumulative concentration–response curve to TFLLR-NH$_2$ in physiological conditions (C) and 24 h after CYP injection (D).

Figure 4

Upper panel: concentration–response curves for TFLLR-NH$_2$-induced contractions of bladder strips *in vitro*. Effect of pretreatment with F16357 or vehicle (DMSO 0.3%). Physiological conditions, $n = 5$ for all concentrations of F16357 and $n = 7$ for vehicle group (A). Pathological conditions, 24 h after CYP injection, $n = 6$ for all concentrations of F16357 and $n = 10$ for vehicle group (B). Lower panel: effect of pretreatment with F16357 or vehicle (DMSO 0.3%) on thrombin 3 U·mL^{-1} incubation followed by TFLLR-NH$_2$ 100 μM-induced contraction of bladder strips *in vitro*. Physiological conditions, $n = 5$ for all groups (C). Pathological conditions, 24 h after CYP injection, $n = 6$ for vehicle group and $n = 5$ for F16357 group (D).

amplitude was about 1.1 g (corresponding to 27% of KCl contraction) and was twofold higher in inflamed tissues compared with control conditions. Pretreatment with F16357 decreased the TFLLR-NH$_2$-induced bladder contraction in a concentration-dependent manner from 10 μM up

to a total blockade at 30 μM ($P < 0.05$ for both) (Figure 4B). The pIC$_{50}$ values of F16357 were 5.32 and 5.07 in control and inflammatory conditions respectively. These results suggest that PAR1 is more involved in this pathological condition and that the potency of F16357 was not modified.

In a separate set of experiments, thrombin (a PAR1 selective protease, 3 U·mL^{-1}) and TFLLR-NH$_2$ (100 μM) induced first a phasic bladder contraction followed by a tonic change with an increase in rhythmic contractions in both physiological and CYP conditions. In physiological conditions (Figure 4C), bladder contractions were around 0.3 g with thrombin and 0.6 g with TFLLR-NH$_2$. F16357 30 μM antagonized both means of stimulation [protease (P = 0.06) and agonist peptide (P < 0.05)]. 24 h after CYP (Figure 4D), thrombin and TFLLR-NH$_2$ contracted the bladder to a larger extent, and the associated micro-contractions during the tonic phases were also increased (not shown). In inflammatory conditions, F16357 30 μM abolished both thrombin- and TFLLR-NH$_2$-induced bladder contraction (P < 0.05 for both activators). These data demonstrate that the bladder PAR1 signalling pathway can be activated by two distinct mechanisms. F16357 suppressed both thrombin- and TFLLR-NH$_2$-induced bladder contractions (P < 0.05) and blocked each agonist-induced increase in micro-contractions in physiological and inflammatory conditions.

Effect of PAR1 blockade on cystometric parameters

Typical traces recorded in control and after CYP injection (150 mg·kg^{-1}, i.p.) are shown in Figure 5A. In both records, the upper trace shows bladder pressure and the lower voided volume. Furosemide injection induced an increase in the diuresis, which resulted in the rapid production of urine, bladder filling and the triggering of a series of several voids. A perfect time match between individual voided volumes and maximal pressures corresponding to micturitions was obtained in all records. The amplitude of the micturition was almost stable throughout the 60 min recording. The pattern of voiding was such that the ICI increased following the furosemide injection and, in the last 30 min, its diuretic effects waned. Interestingly, individual voided volumes were constant (Figure 5A) despite the progressive increase in ICI.

Seven hours after CYP injection, a furosemide pulse induced an increase in the number of micturitions and a decrease in ICI without any modification of the amplitude of bladder contraction (Figure 5B, upper panel) as compared with control. CYP also decreased the mean volume of individual micturitions, as well as the total voided volume within 1 h. F16357 (30 μM) restored the physiological urodynamic profile and mean voided volumes (P < 0.05) (Figure 5C).

Effect of F16357 on urodynamic parameters in rats

In the absence of CYP-induced inflammation, no notable modification of the cystometry parameters was obtained after a single intravesical injection of F16357 30 μM, regardless of the time of furosemide pulse 7 or 24 h (data not shown).

In rats treated with CYP followed by an intravesical injection of vehicle, a furosemide challenge at 7 h resulted in 18 ± 5 micturitions of 0.7 ± 0.2 mL (mean volume of individual micturitions). The intravesical administration of F16357 30 μM reduced the micturition frequency and increased the individual voided volumes to restore the so-called basal urodynamic parameters (P < 0.05 for both); however,
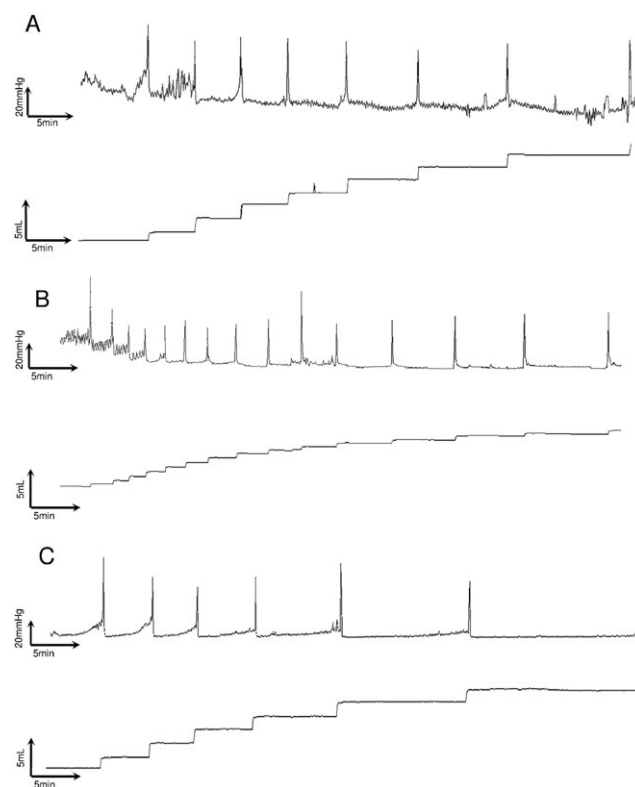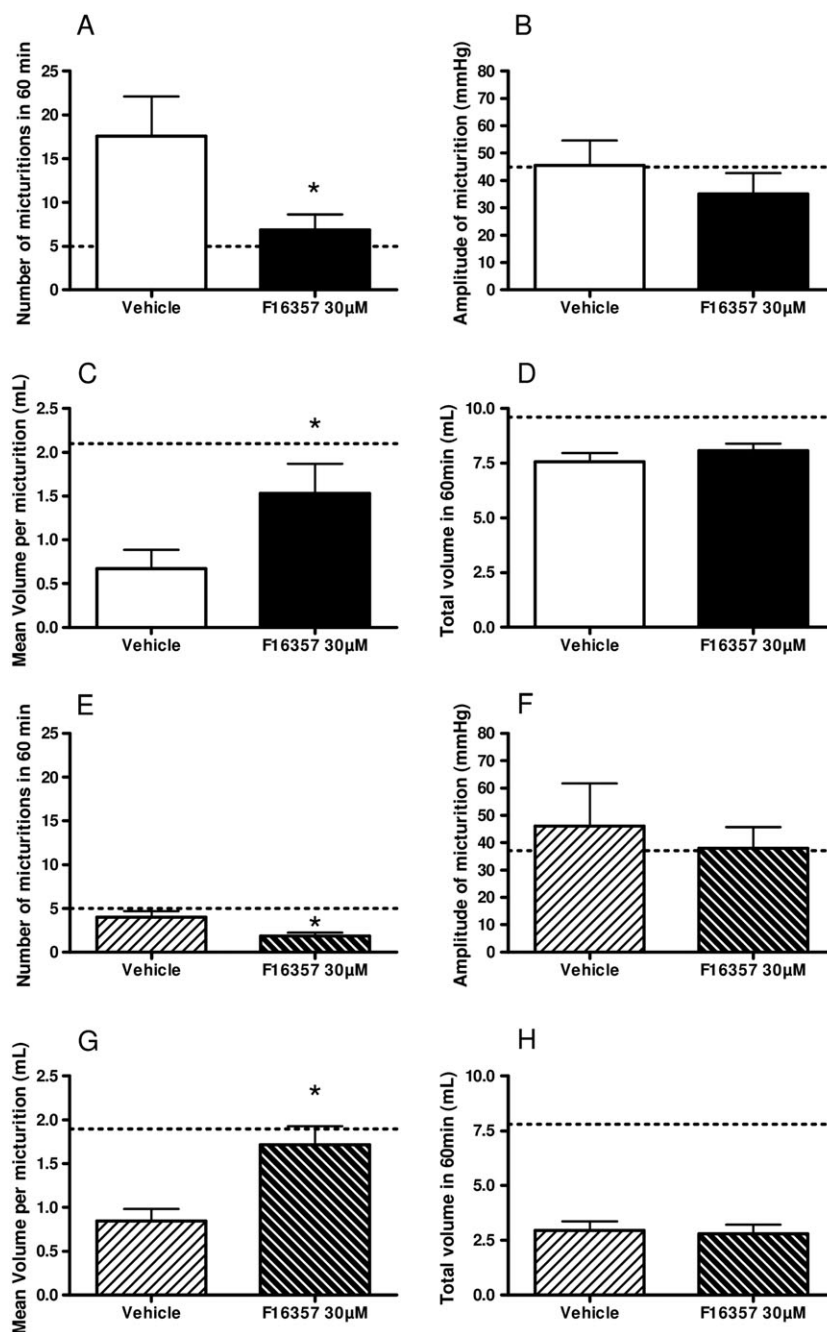

Figure 5

Representative traces of telemetric recording after a pulse of furosemide (10 mg·kg^{-1}, 2 mL·kg^{-1}) in physiological conditions (A), after CYP-induced inflammation (B) and after intravesical administration of F16357 30 μM 2.5 h after CYP injection (C).

the micturition amplitude and the total voided volume were not significantly affected by the F16357 treatment (Figure 6A–D). When the furosemide challenge was repeated at 24 h, the total voided volume was reduced by about 60% when compared with the 7 h time point, thus affecting the number of micturitions (only 4 ± 1). This reduction in total voided volume, despite a reduced voiding frequency, was in accordance with data previously obtained, and corresponded to a significant fall in the rate of urine production as previously reported (Monjotin *et al.*, 2016). The intravesical administration of F16357 30 μM significantly reduced the micturition frequency and increased the individual voided volumes in a comparable magnitude as those at 7 h (P < 0.05). Again, the amplitude of micturition and the total voided volume were not affected by this pharmacological treatment (Figure 6E–H). These data demonstrate that the local treatment of F16357 (30 μM) for 1 h in the bladder lumen was able to reduce the number of micturitions, an effect lasting for up to 22 h post-infusion.

Effect of lidocaine on urodynamic parameters in CYP-treated rats

After the 7 h furosemide pulse, lidocaine 2% reduced the number of micturitions and increased the mean individual voided volumes when compared with vehicle (P < 0.05), without
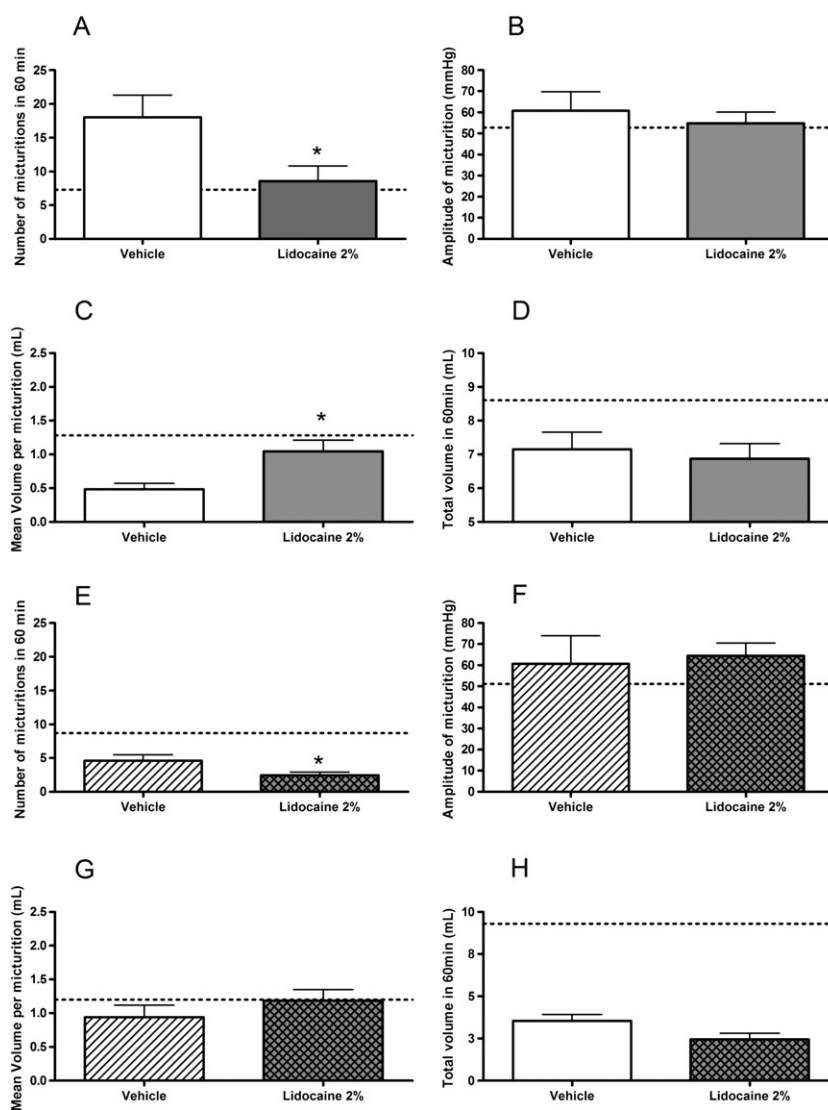
Figure 6

Effect of intravesical administration of vehicle ($n = 7$) or F16357 30 μM ($n = 6$) (0.6 mL for 1 h) 7 h (A-D) and 24 h (E-H) on the number of micturitions (A and E), the amplitude of micturition (B and F), the mean voided volume per micturition (C and G) and the total voided volume in 1 h after furosemide pulse (D and H). Dotted line represents the mean values obtained with intravesical infusion of vehicle in physiological conditions ($n = 4$).

affecting the other urodynamic parameters (Figure 7A–D). When the furosemide challenge was retested at 24 h, a reduction in the micturition frequency was also observed, and the other parameters measured were not affected significantly by the lidocaine 2% treatment (Figure 7E–H). These data support the idea that reducing sensation could be a key component for alleviating the urodynamic disturbances mediated by a powerful inflammatory agent in this rat IC model.

Discussion

The present study suggests that PAR1 may be a novel therapeutic in the management of IC. Furthermore, pharmacological actions of a selective PAR1 antagonist, F16357 (Perez *et al.*, 2009; Ramachandran *et al.*, 2012), may be particularly useful in the alleviation of IC symptoms. Firstly, the data demonstrate that PAR1 expression increases in inflammatory

Figure 7

Effect of intravesical administration of vehicle ($n = 6$) or lidocaine 2% ($n = 7$) (0.3 mL for 1 h) 7 h (A-D) and 24 h (E-H) on the number of micturitions (A and E), the amplitude of micturition (B and F), the mean voided volume per micturition (C and G) and the total voided volume in 1 h after furosemide pulse (D and H). Dotted line represents the mean values obtained with intravesical infusion of vehicle in physiological conditions ($n = 9$).

conditions in the rat urothelium, in the well-established model of haemorrhagic cystitis induced by CYP. Secondly, functional studies demonstrate a physiological response involving PAR1 both in isolated bladders and in conscious freely moving rats. Interestingly, the compound F16357 exhibited a concentration-dependent antagonism of PAR1 and demonstrated a clear improvement of the symptoms of bladder sensation induced by CYP.

Proteases like tryptase (Boucher *et al.*, 1995; Okragly *et al.*, 1999) or neutrophil elastase (Kuromitsu *et al.*, 2008) are released during inflammation, and their levels are found to be increased in urine from IC patients. Thrombin, another serine protease with a high affinity for PAR1, plays an important role in the induction of inflammation and pain (Vergnolle, 2009). In rat bladder, the distribution of PARs is well established for PAR2, PAR3 and PAR4, but PAR1 has yet to be further characterized (D'Andrea *et al.*, 2003; Moffatt, 2007; Vera

et al., 2010). Nevertheless, the presence of PAR1 was confirmed in rat bladder by Vera in 2010 and has recently been shown to be involved in bladder pain by Kouzoukas in 2015, but its role in bladder function has yet to be established (Vera *et al.*, 2010; Kouzoukas *et al.*, 2015). In human bladder cells (Urotsa), all four subtypes of PAR have been well characterized (Vera *et al.*, 2010).

The first goal of this work was to study the modulation of PAR1 expression in the rat bladder wall in both physiological and inflammatory conditions. The present findings demonstrate that PAR1 is only present in some urothelial cells under control, non-inflammatory conditions. However, 24 h after CYP injection, the urothelium is damaged, and the remaining urothelial cells were also found to express PAR1. No PAR1 was found in *lamina propria* despite expansion of the interstitial space associated with the inflammation. These results in rat bladders are different from those in mouse in which inflammation decreased the PAR1 expression

(D'Andrea *et al.*, 2003). The observations obtained here demonstrate that local administration of a PAR1 antagonist (F16357) during the acute phase of the inflammation (i.e. 2.5 h after CYP injection) (Lanteri-Minet *et al.*, 1995) limits the urothelial damage and eliminates the increased expression of PAR1-IR. However, it does not appear to moderate the expansion of the *lamina propria*.

Moreover, PAR1 is involved in bladder pain in animal models (Kouzoukas *et al.*, 2015). These findings associated with the immunostaining results demonstrate the potential of a PAR1 antagonist, namely, F16357, in the pathophysiology and treatment of IC.

The second set of experiments demonstrates a functional role for PAR1 in bladder contractions after stimulation by either an endogenous protease (i.e. thrombin) or an agonist peptide (i.e. TFLLR-NH$_2$) (Vergnolle, 2009).The increased activity of PAR1 was demonstrated in bladder inflammation, in line with the increased expression of the target. To the best of our knowledge, the functional implication of PAR1 has never been reported in rat bladder contractility, and PAR1 effects are selectively and concentration-dependently antagonized by F16357. In the present experimental conditions, a smaller bladder contraction was obtained with thrombin than with TFLLR-NH$_2$, which could be explained either by the presence of natural anti-protease or by an off-target effect (Benezra *et al.*, 1993; Lafleur *et al.*, 2001; Tran and Stewart, 2003). At the concentrations tested, a difference in efficacy between the two agonists is not related to an insufficient concentration of thrombin because 3 UI·mL^{-1} was supramaximal (data not shown). Another explanation could also be related to a difference in the mechanism of PAR1-induced activation because TFLLR-NH$_2$ does not display any enzymatic activity. Moreover, rhythmic contractions were reported by Nakahara in 2004 after trypsin-induced bladder contractions in CYP-treated rats (Nakahara *et al.*, 2004). In the present work, thrombin and TFLLR-NH$_2$ also induced rhythmic detrusor contractions that were reduced by F16357. All these data confirm the role of PARs and especially PAR1 in rhythmic contractions. In these conditions, the concentration-dependent antagonism induced by F16357 on detrusor contractility demonstrates that PAR1 is a very interesting target for the management of bladder overactivity and the exacerbation of the bladder sensitivity described in IC patients (Grover *et al.*, 2011). Nevertheless, in order to evaluate the involvement of bladder sensitivity in the bladder contractility, the relationship between PAR1 expression in the urothelium and detrusor function warrants further investigations.

In the next part of this study, the effects of F16357 were examined in an integrative animal model of IC induced by CYP. As described previously (Monjotin *et al.*, 2016), radiotelemetry enables continuous recording of urodynamic parameters in fully unrestrained conditions in conscious animals. The bladder is not filled artificially with saline but urine following as part of an endogenous diuresis. Consequently, bladder filling and emptying operate in a more physiological condition (Buyuknacar *et al.*, 2008; Andersson *et al.*, 2011). As a result, the timing of a void is determined by the animal, a conscious decision, and not only by activation of reflexes when the bladder is full. The decision of the animal to void therefore involves the integration of multiple inputs: painful sensation and volume sensations (Eastham and Gillespie, 2013).

Bladder function was recorded at the critical time periods after CYP injection (Dornelles *et al.*, 2014). In acute inflammatory conditions (i.e. 7 h after CYP injection), furosemide, a loop diuretic with a short half-life (update ANSM November 2010), greatly increased the number of micturitions and decreased the voided volume per micturition compared with the physiological state. This change in the voiding pattern is consistent with the idea that the introduction of painful bladder sensations, as a result of the CYP-induced cystitis, contributes to the decision to void (Cox, 1979; Saitoh *et al.*, 2010; Pessina *et al.*, 2015). F16357 was tested in this stringent rat model of IC, in order to evaluate the effect of a PAR1 antagonist. These telemetric data demonstrate a very clear beneficial effect of a short and local administration of F16357 on voiding pattern and urodynamic parameters, thus supporting an hypothesis for the involvement of a PAR component (Dattilio and Vizzard, 2005; Vergnolle, 2009), especially PAR1 in the bladder pain sensation (Kouzoukas *et al.*, 2015). These beneficial effects are maintained during the chronic phase of inflammation up to 24 h (Jezernik *et al.*, 2003).

Interestingly, furosemide induced a different effect on urine production at the two different times of recording; 24 h after CYP injection, the number of voids was reduced markedly in all groups. We have previously reported the same results after water loading instead of the furosemide pulse (Monjotin *et al.*, 2016), thus eliminating a possible interaction between furosemide and CYP or its metabolites, or a loss of the pharmacological efficacy of furosemide during the second pulse. These observations could probably be induced by a major effect of CYP on kidney function (Kim *et al.*, 2011).

Local administration of lidocaine, a therapeutic option for IC management (Henry *et al.*, 2015), was evaluated, and comparable results with F16357 in amplitude and duration were obtained. In humans, intravesical instillations of lidocaine 2% may interrupt the self-perpetuating neuro-inflammatory cycle presented in IC (Henry *et al.*, 2015). In the current experimental model, the comparable effects obtained with lidocaine and F16357 confirm the involvement of pain sensation in the modification of the voiding pattern. Collectively, these results show that PAR1 antagonism plays a key role in the control of bladder pain either by a direct effect on receptor or by an indirect mechanism with inhibition of some inflammatory cytokines such as MIF (Kouzoukas *et al.*, 2015).

Finally, the urodynamic and immunohistochemistry results suggest an effect of F16357 on the urothelial reconstruction, but further explorations (especially on the kinetic effect of F16357) are required. Several hypotheses can be proposed, such as the role of PAR1 antagonism in the acceleration of the urothelial repair, the prevention of urothelium damage or a combination of both.

Conclusion

This work has demonstrated the presence of PAR1 in the rat bladder and its involvement in bladder function and sensation. The local administration of the novel selective PAR1 antagonist F16357 elicits robust and durable effects on bladder contractility, urodynamics and bladder pain sensation. Hence, F16357 could represent an interesting candidate for

IC/PBS treatment because it improves most of the pathological features, namely, pelvic pain, inflammation and detrusor dysfunction.

Acknowledgements

Author contributions

N.M. performed the research, designed the research study, analysed the data, supervised the study and wrote the paper. J.G. designed the research study, analysed the data, provided critical discussions and approved the version to be published. M.F. performed the research and analysed the data. B.L.G. provided critical discussions and approved the version to be published. D.J. analysed the data, provided critical discussions and approved the version to be published. N.V. supervised the study, provided critical discussions and approved the version to be published.

Conflict of interest

N.M., M.F., B.L.G. and D.J. are employees of Institut de Recherche Pierre Fabre. J.G. is a scientific consultant for the Institut de Recherche Pierre Fabre.

Declaration of transparency and scientific rigour

This Declaration acknowledges that this paper adheres to the principles for transparent reporting and scientific rigour of preclinical research recommended by funding agencies, publishers and other organisations engaged with supporting research.

References

Alexander SP, Davenport AP, Kelly E, Marrion N, Peters JA, Benson HE *et al.* (2015a). The Concise Guide to PHARMACOLOGY 2015/16: G protein-coupled receptors. Br J Pharmacol 172: 5744–5869.

Alexander SPH, Fabbro D, Kelly E, Marrion N, Peters JA, Benson HE *et al.* (2015b). The Concise Guide to PHARMACOLOGY 2015/16: Enzymes. Br J Pharmacol 172: 6024–6109.

Andersson KE, Soler R, Fullhase C (2011). Rodent models for urodynamic investigation. NeurourolUrodyn 30: 636–646.

Auge C, Chene G, Dubourdeau M, Desoubzdanne D, Corman B, Palea S *et al.* (2013). Relevance of the cyclophosphamide-induced cystitis model for pharmacological studies targeting inflammation and pain of the bladder. Eur J Pharmacol 707: 32–40.

Benezra M, Vlodavsky I, Ishai-Michaeli R, Neufeld G, Bar-Shavit R (1993). Thrombin-induced release of active basic fibroblast growth factor-heparan sulfate complexes from subendothelial extracellular matrix. Blood 81: 3324–3331.

Boucher W, El-Mansoury M, Pang X, Sant GR, Theoharides TC (1995). Elevated mast cell tryptase in the urine of patients with interstitial cystitis. Br J Urol 76: 94–100.

Buyuknacar HS, Kumcu EK, Gocmen C, Onder S (2008). Effect of phosphodiesterase type 4 inhibitor rolipram on cyclophosphamide-induced cystitis in rats. Eur J Pharmacol 586: 293–299.

Cox PJ (1979). Cyclophosphamide cystitis–identification of acrolein as the causative agent. Biochem Pharmacol 28: 2045–2049.

Curtis MJ, Bond RA, Spina D, Ahluwalia A, Alexander SP, Giembycz MA *et al.* (2015). Experimental design and analysis and their reporting: new guidance for publication in BJP. Br J Pharmacol 172: 3461–3471.

D'Andrea MR, Saban MR, Nguyen NB, Andrade-Gordon P, Saban R (2003). Expression of protease-activated receptor-1, -2, -3, and -4 in control and experimentally inflamed mouse bladder. Am J Pathol 162: 907–923.

Dattilio A, Vizzard MA (2005). Up-regulation of protease activated receptors in bladder after cyclophosphamide induced cystitis and colocalization with capsaicin receptor (VR1) in bladder nerve fibers. J Urol 173: 635–639.

De Vries L, Palmier C, Finana F, Le Grand B, Perez M, Cussac D (2006). Pharmacological characterization of protease activated receptor-1 by a serum responsive element-dependent reporter gene assay: major role of calmodulin. Biochem Pharmacol 71: 1449–1458.

Dery O, Corvera CU, Steinhoff M, Bunnett NW (1998). Proteinase-activated receptors: novel mechanisms of signaling by serine proteases. Am J Physiol 274: C1429–C1452.

Dornelles FN, Andrade EL, Campos MM, Calixto JB (2014). Role of CXCR2 and TRPV1 in functional, inflammatory and behavioural changes in the rat model of cyclophosphamide-induced haemorrhagic cystitis. Br J Pharmacol 171: 452–467.

Eastham JE, Gillespie JI (2013). The concept of peripheral modulation of bladder sensation. Organogenesis 9: 224–233.

Grover S, Srivastava A, Lee R, Tewari AK, Te AE (2011). Role of inflammation in bladder function and interstitial cystitis. Ther Adv Urol 3: 19–33.

Hanno PM, Erickson D, Moldwin R, Faraday MM (2015). Diagnosis and treatment of interstitial cystitis/bladder pain syndrome: AUA guideline amendment. 193: 1545–1553.

Henry RA, Morales A, Cahill CM (2015). Beyond a simple anesthetic effect: lidocaine in the diagnosis and treatment of interstitial cystitis/bladder pain syndrome. Urology 85: 1025–1033.

Hu VY, Zvara P, Dattilio A, Redman TL, Allen SJ, Dawbarn D *et al.* (2005). Decrease in bladder overactivity with REN1820 in rats with cyclophosphamide induced cystitis. J Urol 173: 1016–1021.

Jezernik K, Romih R, Mannherz HG, Koprivec D (2003). Immunohistochemical detection of apoptosis, proliferation and inducible nitric oxide synthase in rat urothelium damaged by cyclophosphamide treatment. Cell Biol Int 27: 863–869.

Kilkenny C, Browne W, Cuthill IC, Emerson M, Altman DG (2010). Animal research: reporting in vivo experiments: the ARRIVE guidelines. Br J Pharmacol 160: 1577–1579.

Kim S, Jo CH, Park JS, Han HJ, Kim GH (2011). The role of proximal nephron in cyclophosphamide-induced water retention: preliminary data. Electrolyte Blood Press 9: 7–15.

Kouzoukas DE, Meyer-Siegler KL, Ma F, Westlund KN, Hunt DE, Vera PL (2015). Macrophage migration inhibitory factor mediates PAR-induced bladder pain. PLoS One 10: e0127628.

Kuromitsu S, Yokota H, Hiramoto M, Morita S, Mita H, Yamada T (2008). Increased concentration of neutrophil elastase in urine from patients with interstitial cystitis. Scand J Urol Nephrol 42: 455–461.

Lafleur MA, Hollenberg MD, Atkinson SJ, Knauper V, Murphy G, Edwards DR (2001). Activation of pro-(matrix metalloproteinase-2) (pro-MMP-2) by thrombin is membrane-type-MMP-dependent in human umbilical vein endothelial cells and generates a distinct 63 kDa active species. Biochem J 357: 107–115.

Lanteri-Minet M, Bon K, De Pommery J, Michiels JF, Menetrey D (1995). Cyclophosphamide cystitis as a model of visceral pain in rats: model elaboration and spinal structures involved as revealed by the expression of c-Fos and Krox-24 proteins. Exp Brain Res 105: 220–232.

Lazareno S, Birdsall NJ (1993). Estimation of antagonist Kb from inhibition curves in functional experiments: alternatives to the Cheng–Prusoff equation. Trends Pharmacol Sci 14: 237–239.

Lecci A, Birder LA, Meini S, Catalioto RM, Tramontana M, Giuliani S et al. (2000). Pharmacological evaluation of the role of cyclooxygenase isoenzymes on the micturition reflex following experimental cystitis in rats. Br J Pharmacol 130: 331–338.

McGrath JC, Lilley E (2015). Implementing guidelines on reporting research using animals (ARRIVE etc.): new requirements for publication in BJP. Br J Pharmacol 172: 3189–3193.

Moffatt JD (2007). Proteinase-activated receptors in the lower urinary tract. Naunyn Schmiedebergs Arch Pharmacol 375: 1–9.

Monjotin N, Farrie M, Vergnolle N, Le Grand B, Gillespie J, Junquero D (2016). Bladder telemetry: A new approach to evaluate micturition behavior under physiological and inflammatory conditions. Neurourol Urodyn. doi: 10.1002/nau.22970.

Nakahara T, Kubota Y, Saito M, Sakamoto K, Ishii K (2004). Protease-activated receptor-2-mediated contraction of urinary bladder is enhanced in cyclophosphamide-treated rats. Naunyn Schmiedebergs Arch Pharmacol 369: 212–219.

Okragly AJ, Niles AL, Saban R, Schmidt D, Hoffman RL, Warner TF et al. (1999). Elevated tryptase, nerve growth factor, neurotrophin-3 and glial cell line-derived neurotrophic factor levels in the urine of interstitial cystitis and bladder cancer patients. J Urol 161: 438–441 ; discussion 441-2.

Perez M, Lamothe M, Maraval C, Mirabel E, Loubat C, Planty B et al. (2009). Discovery of novel protease activated receptors 1 antagonists with potent antithrombotic activity in vivo. J Med Chem 52: 5826–5836.

Pessina F, Capasso R, Borrelli F, Aveta T, Buono L, Valacchi G et al. (2015). Protective effect of palmitoylethanolamide in a rat model of cystitis. J Urol 193: 1401–1408.

Ramachandran R, Noorbakhsh F, Defea K, Hollenberg MD (2012). Targeting proteinase-activated receptors: therapeutic potential and challenges. Nat Rev Drug Discov 11: 69–86.

Saban R, Simpson C, Davis CA, Dozmorov I, Maier J, Fowler B et al. (2007). Transcription factor network downstream of protease activated receptors (PARs) modulating mouse bladder inflammation. BMC Immunol 8: 17.

Saitoh C, Yokoyama H, Chancellor MB, De Groat WC, Yoshimura N (2010). Comparison of voiding function and nociceptive behavior in two rat models of cystitis induced by cyclophosphamide or acetone. NeurourolUrodyn 29: 501–505.

Southan C, Sharman JL, Benson HE, Faccenda E, Pawson AJ, Alexander SP et al. (2016). The IUPHAR/BPS Guide to PHARMACOLOGY in 2016: towards curated quantitative interactions between 1300 protein targets and 6000 ligands. Nucl. Acids Res. 44: D1054–D1068.

Tran T, Stewart AG (2003). Protease-activated receptor (PAR)-independent growth and pro-inflammatory actions of thrombin on human cultured airway smooth muscle. Br J Pharmacol 138: 865–875.

Update ANSM November (2010). In: Medicament ANDSD (ed). Résumé des caractéristiques produit (RCP) Furosemide 20 mg/2 ml, solution injectable.

Vera PL, Wolfe TE, Braley AE, Meyer-Siegler KL (2010). Thrombin induces macrophage migration inhibitory factor release and upregulation in urothelium: a possible contribution to bladder inflammation. PLoS One 5: e15904.

Vergnolle N (2009). Protease-activated receptors as drug targets in inflammation and pain. Pharmacol Ther 123: 292–309.

Wurch T, Colpaert FC, Pauwels PJ (1999). G-protein activation by putative antagonists at mutant Thr373Lys alpha2A adrenergic receptors. Br J Pharmacol 126: 939–948.